ResearchGate

See discussions, stats, and author profiles for this publication at: https://www.researchgate.net/publication/232956676

Block Copolymer Concentration Gradient and Solvent Effects on Nanostructuring of Thin Epoxy Coatings Modified with Epoxidized Styrene–Butadiene–Styrene Block Copolymers

ARTICLE *in* MACROMOLECULES · APRIL 2012

Impact Factor: 5.8 · DOI: 10.1021/ma2018759

CITATIONS
13

READS
74

9 AUTHORS, INCLUDING:

Raquel Fernández
University of Basque Country (UPV/EHU)
37 PUBLICATIONS **331** CITATIONS
SEE PROFILE

Silvia Goyanes
University of Buenos Aires
82 PUBLICATIONS **1,294** CITATIONS
SEE PROFILE

Apostolos Avgeropoulos
University of Ioannina
123 PUBLICATIONS **1,790** CITATIONS
SEE PROFILE

Galder Kortaberria
Universidad del País Vasco / Euskal Herriko U…
91 PUBLICATIONS **857** CITATIONS
SEE PROFILE

Available from: Galder Kortaberria
Retrieved on: 26 January 2016

Macromolecules

Article

pubs.acs.org/Macromolecules

Block Copolymer Concentration Gradient and Solvent Effects on Nanostructuring of Thin Epoxy Coatings Modified with Epoxidized Styrene–Butadiene–Styrene Block Copolymers

José Angel Ramos,[†] Leandro H. Espósito,[†] Raquel Fernández,[†] Iñaki Zalakain,[†] Silvia Goyanes,[‡] Apostolos Avgeropoulos,[§] Nikolaos E. Zafeiropoulos,[§] Galder Kortaberria,[†] and Iñaki Mondragon*,[†]

[†]Group "Materials + Technologies", Department of Chemical and Environmental Engineering, Polytechnic School, University of the Basque Country, Pza. Europa 1, 20018 Donostia-San Sebastian, Spain

[‡]Laboratorio de Polímeros y Materiales Compuestos, Dep Física, FCEN-UBA, Ciudad Universitaria, Pab. 1, C1428EGA, Ciudad Autónoma de Buenos Aires, Argentina

[§]Department of Materials Science and Engineering, University of Ioannina, University Campus - Dourouti, 45110 Ioannina, Greece

ABSTRACT: The gradient on block copolymer concentration through film thickness as well as the effects of casting solvents used on the nanostructuring of a thermosetting epoxy coating modified with an epoxidized poly(styrene-*b*-butadiene-*b*-styrene) (SBS) triblock copolymer was studied by means of atomic force microscopy and attenuated total reflectance infrared spectroscopy. Thin coating films based on a commercial epoxy–amine formulation consisting of diglycidyl ether of bisphenol A and a low-temperature fast curing amine were modified with several amounts of epoxidized SBS triblock copolymer. Toluene and a mixture of tetrahydrofuran and *N*,*N*-dimethylformamide were used as casting solvents. With epoxidation degrees higher than 45 mol % of polybutadiene block nanostructuring was achieved. Fast curing rate of the epoxy/amine system and the comparatively slow evaporation rate of the casting solvent led to a gradient of morphologies through the film cross section owing to the coalescence of small micelles into larger micellar domains in the case of low block copolymer content. For these reasons, different morphologies were also obtained in the midtransverse section of a film with variable thickness. Finally, pseudolamellar nanostructure at high copolymer contents was achieved as confirmed by parallel and perpendicular cuttings to the air/polymer interface.

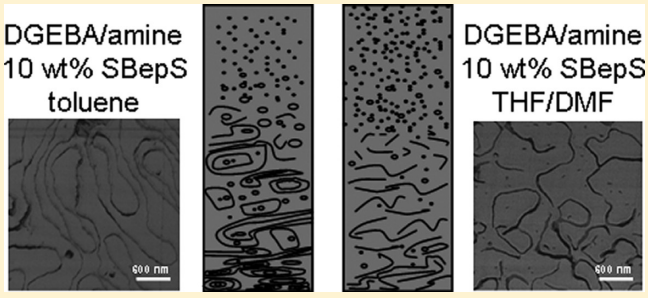

INTRODUCTION

Nanostructured polymers are a unique class of materials that are finding an increasing number of applications.[1] Nanofoamed membranes,[2] nanoreactors,[3] nanotemplates,[4] and nanoporous structures[5] are some of the newest applications of nanostructured materials for microelectronics, nanomaterials synthesis, nanotube fabrication, and antireflection coatings. Thermosetting materials based on epoxy matrices modified with block copolymers are being used increasingly in many studies taking advantage of the capability of generating nanostructured systems as well.[6−9] In addition, the principal limitation of epoxy systems, their poor fracture toughness, can also be improved by the addition of block copolymers to the mixture.[10−13] Historically, fracture toughness improvement was achieved by epoxy modification with thermoplastics or elastomers.[14,15] However, the worsening of other properties, such as transparency, because of the generated macrophase-separated domains compromises the usefulness of those systems. Thus, recently block copolymers have been used as templates for the generation of nanostructured thermosetting matrices.[12−26] The preparation of these materials can further optimize the final properties, maintaining the transparency of the neat materials.[27−32]

Generally, to prepare nanostructured thermosetting materials using block copolymers, at least one of the blocks must be miscible with the matrix and at least one block immiscible.[33−35] However, in the case of styrene–butadiene–styrene (SBS) block copolymer both blocks tend to be immiscible with cured epoxy systems, leading to macrophase-separated material. Thus, in order to promote the compatibility of one of the blocks with the epoxy resin, polybutadiene block must be chemically modified. Serrano et al.[1] reported the synthesis and characterization of epoxidized styrene–butadiene block copolymers as templates for nanostructured thermosets, following the procedure previously reported by Jian and Hay,[36] by using hydrogen peroxide for the oxidation of the double bound of the butadiene units. Previous work of our group reported the effect of both the extent of epoxidation of polybutadiene blocks and the content of polystyrene phase on the mixture.[37,38] Thus, in general, a transition from spherical micelles to wormlike micelles and then to vesicles occurs with the decrease of the epoxy miscible

Received: August 17, 2011
Revised: January 13, 2012
Published: January 27, 2012

ACS Publications © 2012 American Chemical Society

dx.doi.org/10.1021/ma2018759 | *Macromolecules* 2012, 45, 1483–1491

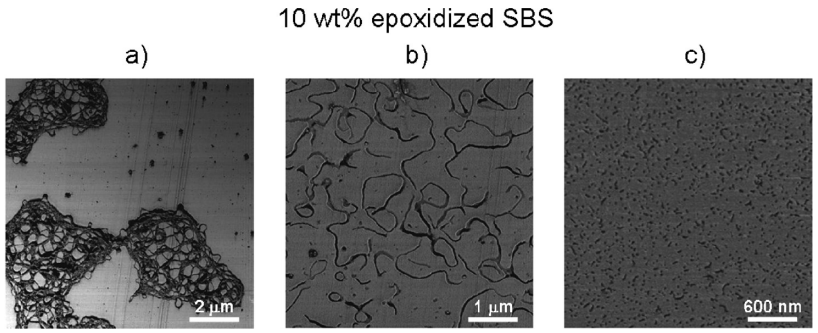

Figure 1. TM-AFM phase images of epoxy mixtures modified with 10 wt % SBS triblock copolymer, epoxidized to different extents, cast in a THF/DMF 1:1 mixture: (a) 37 mol %, image 10 × 10 μm; (b) 46 mol %, image 5 × 5 μm; (c) 52 mol %, image 3 × 3 μm. Images in the midtransverse section of a 240 μm film thickness.

block and/or the increase of the epoxy immiscible block,[27] while for epoxidation extents of the block copolymer higher than the threshold required for miscibility with the epoxy system,[37] long-range ordered nanostructures evoluting from spherical to hexagonally packed cylinders and even lamellas as copolymer content increased are achieved.[39,40]

On the other hand, in the case of thin films, the influence of both solvent used for casting and film thickness should be taken into account in the development of morphology. Hermel-Davidock et al.[26] observed morphology differences in epoxy thermosets modified with poly(ethylene oxide)-*block*-poly(ethylene-*alt*-propylene) (PEO−PEP) cast with two different solvents, acetone and tetrahydrofuran. Acetone, as poorer solvent than tetrahydrofuran for PEO block, can induce the collapse of the micelle corona chains toward the interface to minimize the interfacial tension by adopting a cylindrical morphology instead of spherical micelles. Furthermore, the influence of the amount of a selective solvent in the final morphology when a mixture of solvents is used has been reported by other authors for block copolymers showing morphology transitions from spherical micelles to vesicles.[41−44]

Because of the limited literature on the subject, the aim of this work has been the study of the gradient on copolymer segregation through film thickness and the effects of casting solvents on the resultant microphase-separated morphology achieved in the block copolymer modified epoxy thin films. In this context, the effects of the selectivity of two solvent systems, toluene and the solvent mixture tetrahydrofuran/*N*,*N*-dimethylformamide, on the nanostructured morphology have been studied.

EXPERIMENTAL SECTION

The block copolymer was a linear SBS triblock copolymer, C540, with 60 wt % PB, kindly supplied by Repsol-YPF. The number-average molar mass was 75 000 g mol^{-1}. The epoxidation reaction was carried out using hydrogen peroxide in the presence of an *in situ* prepared catalyst in a water/dichloroethane biphasic system. The details of the reaction are described elsewhere.[1,36] The degree of epoxidation is represented in mol % with respect to PB double bonds. The epoxy monomer used was a diglycidyl ether of bisphenol A (DGEBA) with epoxide equivalent weight of 184−190, supplied by Hexion. The hardener was an aliphatic fast curing amine mixture, composed by *N*-aminoethylpiperazine, *m*-xylylenediamine, and benzyl alcohol, particularly suited to low-temperature conditions, Ancamine 2500, supplied by Air Products. The mixtures were prepared with a weight ratio of 100/58 (epoxy/hardener). Toluene, tetrahydrofuran (THF), and *N*,*N*-dimethylformamide (DMF) used as casting solvents were supplied by Sigma-Aldrich. The mixtures were prepared in three steps. First, the epoxidized block copolymer and DGEBA resin were dissolved in the casting solvent with magnetic stirring. Next, the hardener was added to the mixture at room temperature for 5 min. Finally, the samples were cured in open parallelepipedic polytetrafluorethylene (PTFE) molds at 70 °C for 1 h and postcured at 135 °C for 1 h.

Atomic force microscopy (AFM) topography and phase images of the samples were recorded in tapping mode in air at room temperature by using a scanning probe microscope (Nanoscope IV, Dimension 3100 from Digital Instruments). Phosphorus (n) doped single-beam cantilever (125 μm length) silicon probes having a tip's nominal radius of curvature of 5−10 nm were used. A typical scan rate during recording was 1 Hz. Samples of cured mixtures were prepared using an ultramicrotome (Leica Ultracut R) equipped with a diamond knife.

Infrared spectra were taken using a Nicolet Nexus 670 (FTIR) spectrometer equipped with a single horizontal golden gate attenuated total reflectance (ATR) cell. The internal reflection element was ZnSe with refractive index of 2.4. Spectra were recorded using a spectral width ranging from 800 to 4000 cm^{-1}, with 4 cm^{-1} resolution and an accumulation of 32 scans.

RESULTS AND DISCUSSION

In order to promote chemical compatibilization between the block copolymer and the epoxy matrix, SBS triblock copolymer was epoxidized at different temperatures and times of reaction. Degrees of epoxidation ranging from 35 to 57 mol % of epoxidized polybutadiene units were achieved. Milder conditions produced lower percentages of modification. The degree of epoxidation was calculated by integration of signals using ^{1}H nuclear magnetic resonance (^{1}H NMR) spectra.[37]

Before curing, all the mixtures formed by DGEBA resin, hardener, randomly epoxidized SBS triblock copolymer, and the casting solvent were homogeneous and transparent or translucent, indicating that micro- or macrophase separation occurred before curing for high (>45 mol %) or low (37 mol %) degrees of epoxidation of polybutadiene block, respectively. This fact seems to be related with the degree of miscibility of the epoxidized PB block with the DGEBA/amine system, which is a function of the epoxidation extent. On the other hand, as can be shown in Figure 1 for cured systems modified with 10 wt % of epoxidized block copolymer cast with a 1:1 THF/DMF solvent mixture, a relatively low epoxidation degree (37 mol %) in the PB block led to macrophase separation in the cured system, Figure 1a, because of the larger amount of low-epoxidized PB units that provoked their phase separation before curing. As epoxidation degree increased, microphase-separated

dx.doi.org/10.1021/ma2018759 | *Macromolecules* 2012, 45, 1483−1491

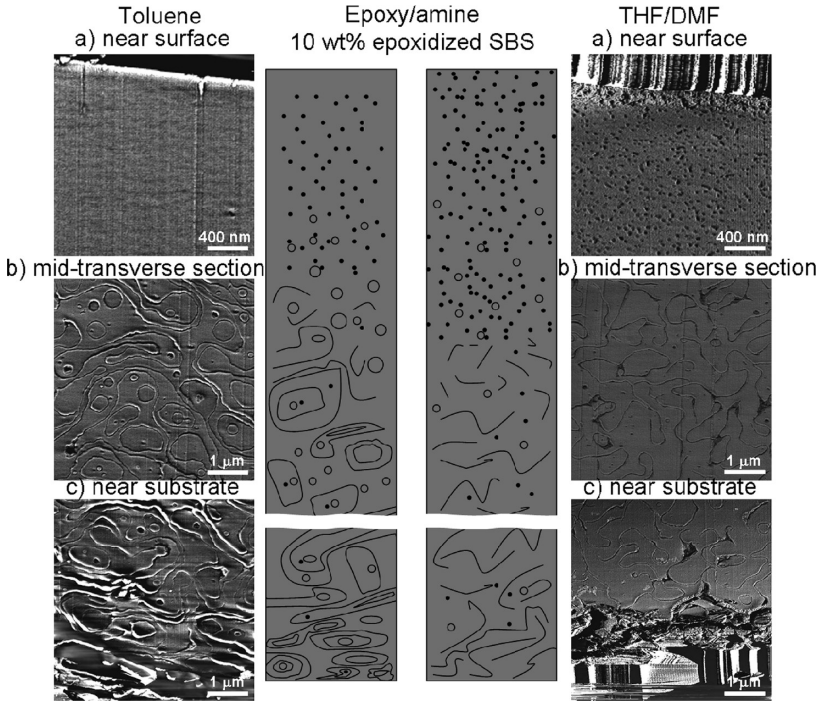

Figure 2. TM-AFM phase images for epoxy mixtures modified with 10 wt % of epoxidized SBS triblock copolymer cast in toluene and THF/DMF 1:1 mixture as a function of the location through a 240 μm film thickness: (a) near the air/polymer interface, images 2 × 2 μm; (b) in the midtransverse section of the film, images 5 × 5 μm; (c) near the polymer/substrate interface, images 5 × 5 μm.

systems could be achieved after curing. Figure 1b shows wormlike micelles corresponding to PS nanodomains (46 mol % epoxidized PB units). Compared with the epoxidation degree previously reported by Ocando et al.[37] needed to overcome the miscibility threshold between epoxidized PB block and epoxy matrix, higher degrees of epoxidation were needed to achieve microphase-separated systems, which is related with the poorer miscibility introduced by the aliphatic fast curing amine used in this work in comparison with the aromatic one in our previous studies.[37,45] Indeed, only systems with high epoxidation degrees (46 mol % or more) showed microphase-separated domains. As we previously reported,[37,45] long-range nanostructuring increased as higher miscibility of epoxidized PB block and epoxy matrix was. This fact can be seen in Figure 1c where the coexistence of spherical micelles with short wormlike micelles due to the larger epoxidation degrees (52 mol % epoxidized PB units) is shown.

With the purpose of evaluating through film thickness the gradient on copolymer segregation and the influence of solvent evaporation on the morphology, two films with constant thickness were analyzed at different regions through film thickness for samples cured with 10 wt % of epoxidized SBS copolymer and toluene and the mixture THF/DMF 1:1 as casting solvents. Ultramicrotomed samples were used for analysis. Results are shown in Figure 2. All samples used herein after have 46 mol % of epoxidation in the butadiene block. In the case of toluene as casting solvent small micelles were achieved near to the air/polymer interface, while in the midtransverse section of the film and near to the polymer/substrate interface the achieved nanostructures corresponded to large-interconnected wormlike micelles coexisting with vesicles and small micelles. The evolution of the morphology along the film thickness passed through several regions from the air/polymer interface to the polymer/substrate interface. Near the air/polymer interface, a region of about 2.2 μm without nanodomains was observed. Inside the film small micelles appeared being more noticeable at a distance of 3.7 μm in depth. At 12.1 μm in depth from the air/polymer interface, small vesicles were detected. At longer distances, up to 18.4 μm the coexistence of small micelles and vesicles, which progressively increased in size, was observed. Then, the beginning of short wormlike micelles formation took place, continuing growing in length until 42.1 μm, where the long wormlike micelles began to interconnect themselves coexisting with small micelles and vesicles. From 54.2 μm, the morphology of large-interconnected wormlike micelles coexisting with small micelles and vesicles remained constant almost up to the interface with the substrate. Finally, near the polymer/substrate interface a flattening of the large-interconnected wormlike micelles was observed. The scheme in Figure 2 simplifies the sequence of the large amount of AFM images obtained along the film thickness. For simplicity, only the regions close to the interfaces and in the mid-transverse section are shown. Similarly, in the case of the mixture with THF/DMF 1:1 as casting solvent, a gradient of morphologies was obtained along the film thickness, with some differences with respect to the case of toluene. The beginning of the nanodomains, as small micelles, started at a close, unmeasurable by AFM images, distance from the air/polymer interface. In addition, the size of these micelles was smaller than in the case of toluene but in higher concentration. This fact was the first evidence of the better solvent quality of the mixture THF/DMF with respect to toluene. Continuing with the evolution of morphology, at a distance of 9.9 μm from the air interface

dx.doi.org/10.1021/ma2018759 | *Macromolecules* 2012, 45, 1483−1491

vesicles began their appearance increasing their size until the next region. At 25.4 μm in depth the formation of short wormlike micelles coexisting with small micelles in larger amount and vesicles in smaller quantity and size than in the case of toluene started. Up to 37.5 μm, long wormlike micelles began their appearance increasing their size and coexisting with small micelles and vesicles until the formation of the morphology, at 49.2 μm in depth, morphology which remained constant until the interface with the substrate. In this case, there was no noticeable flattening of the long wormlike micelles near to the polymer/substrate interface, as in the case of toluene. The no formation of interconnected and closed wormlike micelles appears to be the second evidence of the better solvent quality of the mixture THF/DMF with respect to toluene because of the favored polymer−solvent interactions instead of polymer−polymer ones.[44] As conclusions for both solvents, it seemed that the morphology gradient could be due to the increase of copolymer concentration from the air/polymer interface to the substrate/polymer interface. The progressive increase in copolymer concentration in the region close to the air/polymer interface up to the midsection, the largest region where copolymer concentration was constant, caused the growing of the small micelles by coalescence, leading to the formation of short wormlike micelles which rapidly transformed in small vesicles to minimize the interfacial tension.[26,27] As the increase of copolymer concentration continued, larger structures were achieved. Because of the fast curing rate of the DGEBA/amine system the structures were frozen. Furthermore, the distances from the air/polymer interface to the regions of morphology transitions were similar in both cases: 12.1 and 9.9 μm for vesicles, 18.4 and 25.4 μm for wormlike micelles, 42.1 and 37.5 μm for long-wormlike, 54.2 and 49.2 μm for constant morphology for the casting solvents toluene and THF/DMF 1:1, respectively, indicating that the copolymer segregation was not due to the selected solvent. Thus, we can suggest the preparation of films by solvent evaporation does not necessarily produce the equilibrium morphology but a gradient of morphologies through the film thickness. The higher evaporation rate of solvents close to the air/polymer interface with respect to the midsection of the film decreases the possibility of the small micelles to coalesce and therefore to form larger structures. At longer distances in depth from the air/polymer interface, longer time in contact with the solvent and longer the structures that could be achieved by coalescence.[26,27] From another point of view, the fast curing rate of the used DGEBA/amine system could also freeze the structures before reaching the equilibrium state. So, the whole process of morphology formation through film thickness appears to be a competition of at least curing reaction, solvent evaporation, and coalescence of micelles.

In order to corroborate the presence of copolymer close to the interfaces and also the possible presence of residual solvent in the samples, ATR-FTIR analysis of the air/polymer and polymer/substrate interfaces was carried out. Figure 3 shows ATR-FTIR spectra of the individual components of the mixtures as well as the interfaces spectra and details of the intervals of interest. Slight variation on the bands in the region 1000−900 cm^{-1}, assigned to C═C out-of-plane bending vibration of the aromatic ring of PS block, can be seen owing to variations in block copolymer concentration. Thus, in the case of 30 wt % block copolymer and toluene as casting solvent, a noticeable decrease in the characteristic bands of PS (910 and 967 cm^{-1}) at the air/polymer interface can be seen. The band at 910 cm^{-1} is too close to the nonreacted epoxy group, and therefore it becomes difficult to distinguish this peak;[1] however, the variation in the 967 cm^{-1} band allowed confirming the variation in copolymer concentration. The depth of penetration of the infrared beam into the sample was estimated supposing a refractive index of the samples close to the neat epoxy of 1.57, as supplied by the manufacturer, and ZnSe as internal reflection element at 45°. In the wavenumbers of interest, the depth of penetration was found to be less than 3 μm (2.75 and 2.58 μm for 910 and 967 cm^{-1}, respectively), a value not sufficient to reach enough block copolymer domains to be measurable in the case of toluene as casting solvent and at the air/polymer interface. This fact supported the conclusions extracted from AFM images in Figure 2, which shows the evolution of the morphology through the film thickness, and in which the presence of the nanodomains began at a distance between 2.2 and 3.7 μm from the air interface. As wormlike micelles began from the polymer/substrate interface, they are measurable by ATR-FTIR. Some differences in FTIR spectra between samples cured with toluene or THF/DMF were observed. Thus, for the samples cured with THF/DMF as casting solvent, there were no noticeable differences in the region of 1000−900 cm^{-1} between the spectra of both interfaces, air/polymer and polymer/substrate, indicating the presence of block copolymer close to both interfaces, at a distance less than the depth of penetration of ATR-FTIR of 3 μm.

Other remarkable fact in the case of the system cast with DMF/THF was the presence of residual DMF as confirmed by means of the appearance of new bands in FTIR spectra in the region of 1800−1600 cm^{-1}, related to C═O group stretching vibration of DMF (Figure 3c).

In addition, to confirm the presence or absence of copolymer at the interfaces, Figure 4 shows the morphology at the interfaces, air/polymer and polymer/substrate, for the systems containing 10 wt % of 46 mol % epoxidized SBS triblock copolymer cured with toluene and THF/DMF as casting solvents. Both systems showed similar results. At the air/polymer interface no nanostructuring was achieved, indicating the absence of microphase-separated copolymer in that interface, far in the case of toluene, 2.2 μm, and close in the case of THF/DMF, unmeasurable. However, at the polymer/substrate interface, nanostructuring was suggested between mold imprinted lines, ensuring the presence of microphase-separated copolymer in that interface.

Thus, a conclusion that can be drawn is that AFM images and ATR-FTIR analysis revealed that the block copolymer concentration at the near air/polymer interface was much lower than in the near mold interface.

A similar effect can be observed in a film with variable thickness, from 30 to 240 μm. Figure 5 shows the morphology evolution in the midtransverse section of the film as a function of the thickness for a system containing 20 wt % epoxidized SBS triblock copolymer and cast in a 1:1 mixture of THF and DMF. Images every 10 μm from the lowest film thickness (30 μm) to the highest film thickness (240 μm) were obtained. It should be noted that images were made in the midtransverse section of each thickness of the film.

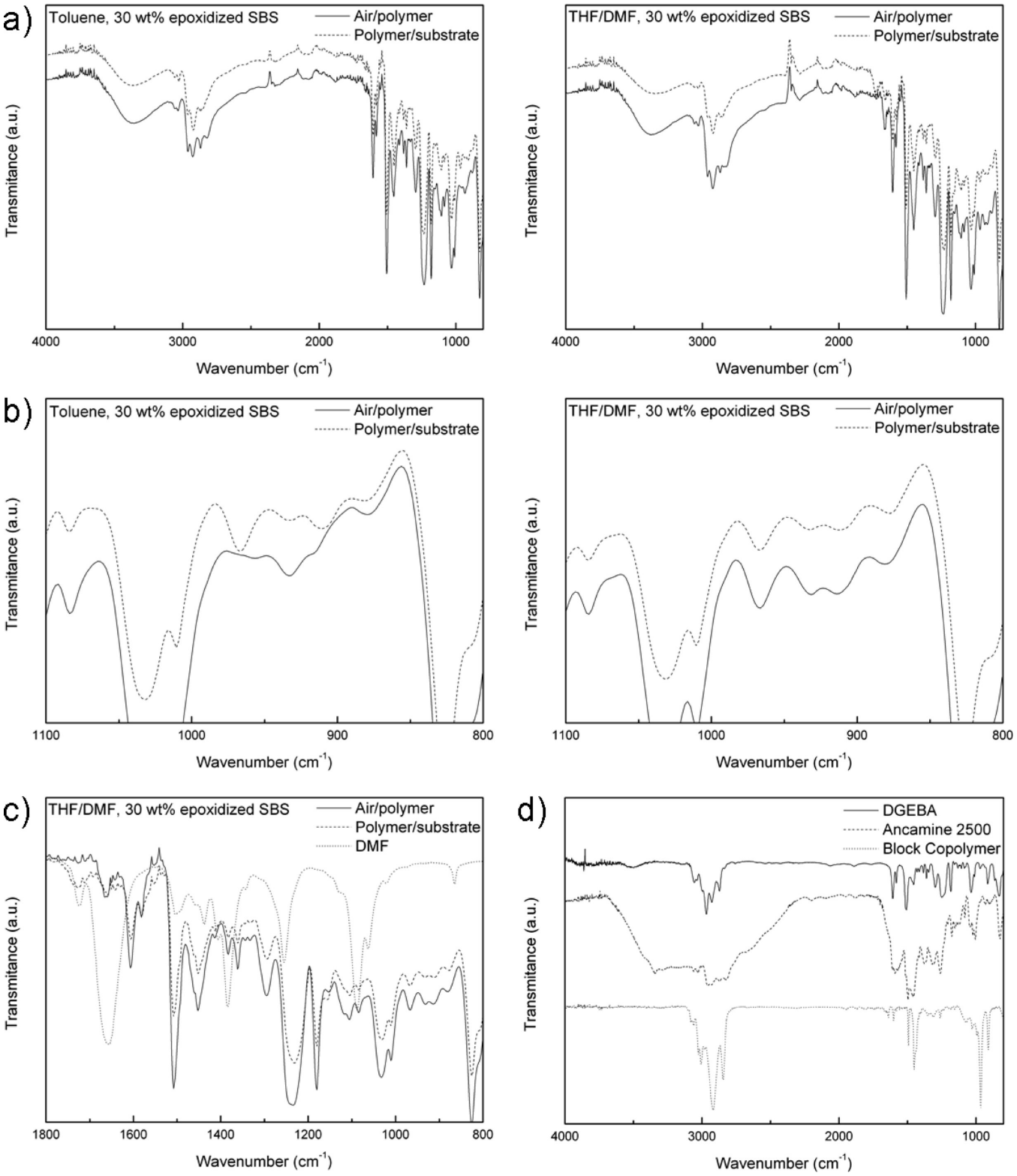

Figure 3. ATR-FTIR spectra of air/polymer and polymer/substrate interfaces of epoxy mixtures modified with 30 wt % of 46 mol % epoxidized SBS triblock copolymer cast in toluene and in THF/DMF 1:1 within the ranges (a) 4000−800, (b) 1100−800, and (c) 1800−800 cm^{-1} only cast in THF/DMF 1:1 and (d) FTIR spectra of individual components of the mixture.

Nevertheless, only four images are reported for simplicity. Spherical micelles coexisting with wormlike micelles were achieved at low thickness. With the increase in thickness, an increase in the length of the wormlike micelles, and a reduction in the amount of spherical micelles was observed. This morphological gradient seems to be due to the gradient in copolymer concentration through the film thickness and the different evaporation rate of solvents. As AFM images

dx.doi.org/10.1021/ma2018759 | *Macromolecules* 2012, 45, 1483−1491

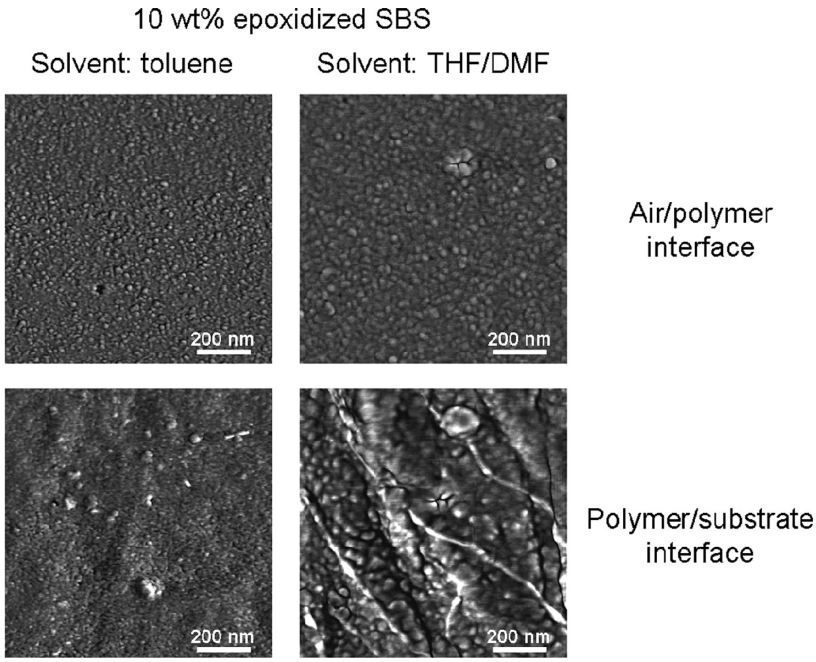

Figure 4. TM-AFM phase images of air/polymer and polymer/substrate interfaces of epoxy mixtures modified with 10 wt % of 46 mol % epoxidized SBS triblock copolymer cast in toluene and in THF/DMF 1:1. Images 1 × 1 μm.

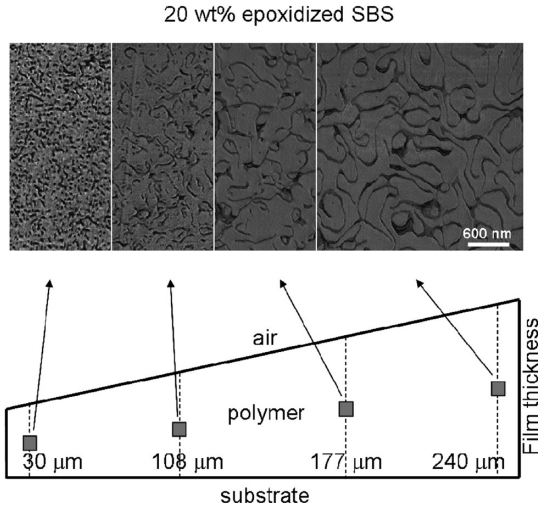

Figure 5. TM-AFM phase images in the transverse section of the film for epoxy mixtures modified with 20 wt % of 46 mol % epoxidized SBS triblock copolymer cast in THF/DMF 1:1 as a function of film thickness. Images 3 × 3 μm.

were taken in the midtransverse section of the film, the higher the film thickness the higher the depth from the air/polymer interface. Thus, the lower the film thickness the higher the influence of copolymer segregation gradient in the midtransverse section of the film. Consequently, the different morphologies due to the copolymer segregation gradient, shown in Figure 2, would be overlapped obtaining almost a unique morphology, which is shown in Figure 5 for the image corresponding to 15 μm depth from the air/polymer interface, corresponding to the midtransverse section of 30 μm film thickness. In addition, the high boiling point of DMF could ease the formation of ordered structures as the system remained longer times with low viscosity. Longer times in contact with the solvent before freezing of the nanostructure at system gelation led to minimization of the interfacial tension of nanodomains. Therefore, larger wormlike micelle morphology was developed by coalescence of spherical micelle structures.[26,27] Hence, shorter domains were achieved at low film thickness due to the faster solvent evaporation, as shown in the image of 30 μm film thickness, as occurred at low film depth in Figure 2. Thus, films thinner than 30 μm would lead to homogeneous nanostructured coatings.

On the other hand, the effect of using different casting solvents on the nanostructure of systems with different amounts of block copolymer was also studied. Figure 6 shows AFM images in the transverse section of thin films for several mixtures cast with a THF/DMF 1:1 mixture as casting solvent. The system modified with 5 wt % epoxidized SBS triblock copolymer showed a combined morphology in which spherical and wormlike micelles with vesicles did coexist. The system with 10 wt % epoxidized block copolymer exhibited the same combined morphology with longer wormlike micelles. Addition of more block copolymer resulted in the decrease of the interfacial area, which yielded to the formation of wormlike micelles by the coalescence of spherical nanodomains.[27,46] Coatings with 20 and 30 wt % epoxidized block copolymer showed interconnected wormlike micelles and more compacted nanostructures than at lower copolymer contents. Finally, microphase separation led to a pseudolamellar nanostructure for 40 wt % triblock copolymer, as the interconnected wormlike microdomains would reduce the interfacial tension by generating planar interfaces, and thereby the long-range ordered lamellar nanostructures were obtained.[35] Similar nanostructures were obtained for samples cured with toluene, as can be seen in Figure 7. However, lamellar nanostructures were achieved at lower contents, i.e., 20−30 wt % of copolymer, due to the solvent quality and the different evaporation rate of toluene and the mixture THF/DMF. In addition, interconnected wormlike micelles were also achieved at lower contents of

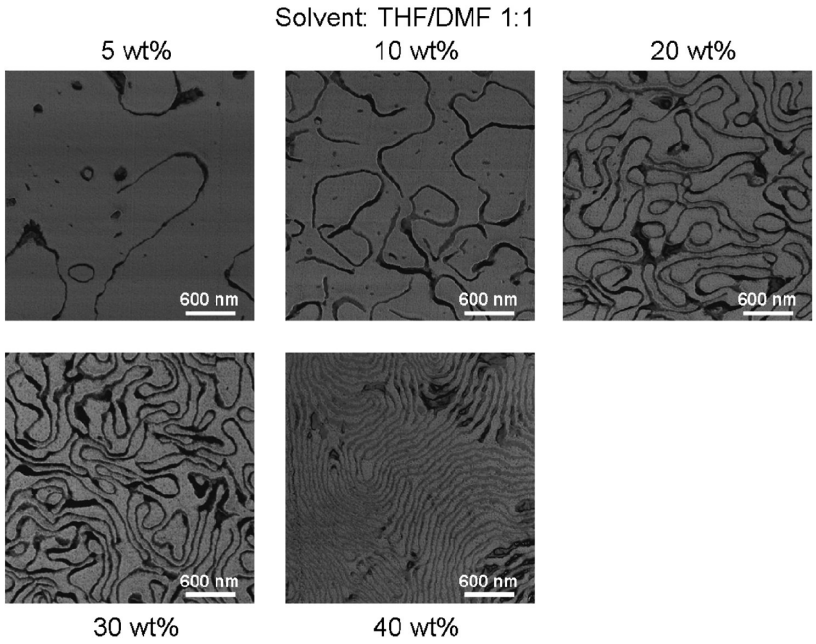

Figure 6. TM-AFM phase images for epoxy mixtures modified with 5, 10, 20, 30, and 40 wt % of 46 mol % epoxidized SBS triblock copolymer cast in THF/DMF 1:1. 3 μm × 3 μm images in the transverse section of a 240 μm film thickness.

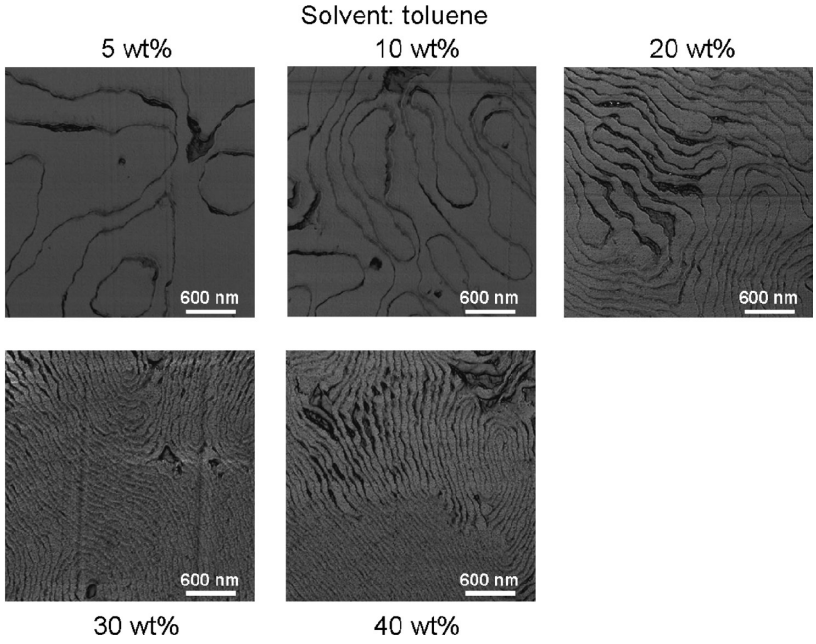

Figure 7. TM-AFM phase images for epoxy mixtures modified with 5, 10, 20, 30, and 40 wt % of 46 mol % epoxidized SBS triblock copolymer cast in toluene. Images 3 × 3 μm in the transverse section of a 240 μm film thickness.

copolymer when cured with toluene. In the mixture with THF/DMF, THF should evaporate during the first stage curing at 70 °C, whereas DMF, because of its highest boiling point, could be reserved in the coatings until the curing reaction was completed. Therefore, it is proposed that the rate of solvent evaporation could significantly affect the kinetics of curing reaction, and thus the morphologies should be influenced. However, although DMF should allow longer times to achieve ordered structures, it seemed that toluene had poorer solvent quality than the THF/DMF mixture. In this study, the individual evaluation of the effect of evaporation rate or the solvent quality was not carried out, so it is suggested that both effects increased polymer−polymer interactions instead of polymer−solvent ones, thus leading to long-range order nanostructures at lower copolymer contents.[44]

In order to analyze the formed nanostructures in all directions, films were cut in two different directions, parallel and perpendicular to the air/polymer interface, and thereafter AFM images in the transverse section of the film were obtained. Figure 8 shows similar nanostructures for two copolymer contents in both cutting directions for the system cast with toluene. Lamellar nanostructures (20 and 30 wt %) appeared in both directions, thus confirming that nanostructures were pseudolamellar instead of cylindrical.

dx.doi.org/10.1021/ma2018759 | *Macromolecules* 2012, 45, 1483−1491

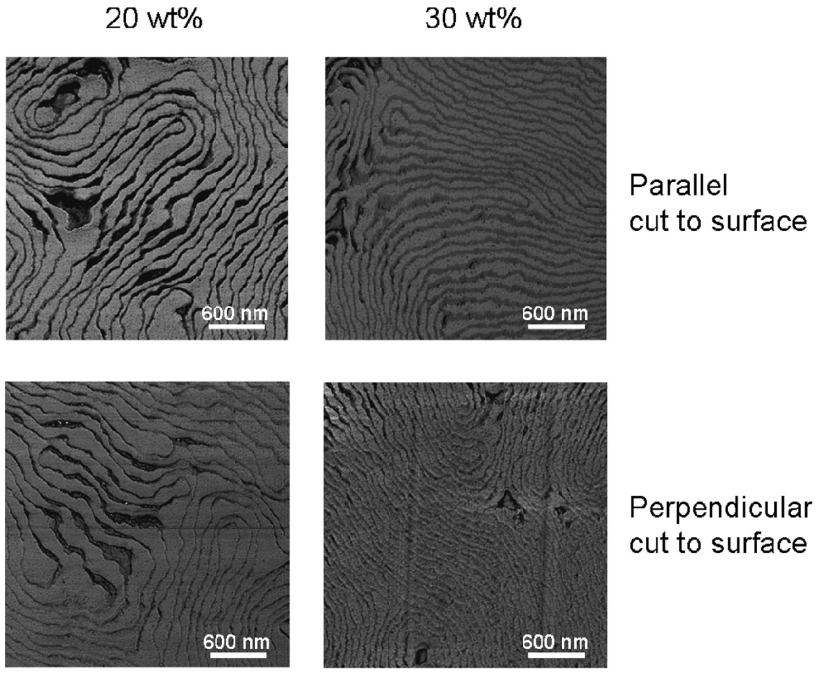

Figure 8. TM-AFM phase images for epoxy mixtures modified with 20 and 30 wt % of epoxidized SBS triblock copolymer cast in toluene as casting solvent for two different directions: top - parallel and bottom - perpendicular cuts to the air/polymer interface. Image 3 × 3 μm in the midsection of a 240 μm film thickness.

■ CONCLUSIONS

A morphological study of the gradient on block copolymer concentration through film thickness and the effects of casting solvents on nanostructuring of an epoxy thin coating system modified with a block copolymer was carried out by atomic force microscopy. A poly(styrene-*b*-butadiene-*b*-styrene) triblock copolymer was randomly epoxidized to compatibilize the butadiene block with the epoxy system. A degree of epoxidation higher than 45 mol % epoxidized polybutadiene units was needed to obtain nanostructured materials.

Owing to the differential segregation of the copolymer through the whole thickness of the film, a gradient of morphologies, which was fixed by the fast curing rate and the relatively slow evaporation rate of solvents, was obtained. By attenuated total reflectance infrared spectroscopy, the absence of block copolymer near the air/polymer interface in the system cast with toluene was verified. Analysis of a film with variable thickness revealed that for thin films morphology gradient was not evident due to the overlap of the different regions with different copolymer concentrations and the faster solvent evaporation which would lead to a homogeneous film. In addition, the poorer solvent quality of toluene in comparison with the mixture of tetrahydrofuran and *N*,*N*-dimethylformamide allowed to achieve pseudolamellar nanostructures at lower copolymer contents; these structures were confirmed by parallel cuttings to the air/polymer interface, which showed similar morphologies which dismissed cylindrical morphology.

■ AUTHOR INFORMATION

Corresponding Author

*E-mail: inaki.mondragon@ehu.es.

Notes

The authors declare no competing financial interest.

■ ACKNOWLEDGMENTS

Financial support from the EU (Carbon nanotube confinement strategies to develop novel polymer matrix composites, POCO, FP7-NMP-2007, CP-IP 213939-1), from the Basque Country Government (Inanogune IE 08-225, Inanogune IE 09-243, Grupos Consolidados IT-365-07), and from the Ministry of Education and Innovation (MAT 2009-06331) is gratefully acknowledged. Moreover, we are grateful to "Macrobehavior - Mesostructure - Nanotechnology" SGIker unit of the UPV/EHU.

■ REFERENCES

(1) Serrano, E.; Larrañaga, M.; Remiro, P. M.; Mondragon, I.; Carrasco, P. M.; Pomposo, J. A.; Mecerreyes, D. *Macromol. Chem. Phys.* **2004**, *205*, 987−996.
(2) Hong, S. M.; Hwang, S. S. *J. Appl. Polym. Sci.* **2006**, *100*, 4964−4971.
(3) Shi, X.; Shen, M.; Möhwald, H. *Prog. Polym. Sci.* **2004**, *29*, 987−1019.
(4) Fu, J.; Cherevko, S.; Chung, C.-H. *Electrochem. Commun.* **2008**, *10*, 514−518.
(5) Joo, W.; Park, M. S.; Kim, J. K. *Langmuir* **2006**, *22*, 7960−7963.
(6) Grubbs, R. B.; Dean, J. M.; Bates, F, S. *Macromolecules* **2001**, *34*, 8593−8595.
(7) Guo, Q.; Thomann, R.; Gronski, W.; Thurn-lbrecht, T. *Macromolecules* **2002**, *35*, 3133−3144.
(8) Guo, Q.; Thomann, R.; Gronski, W.; Staneva, R.; Ivanova, R.; Stühn, B. *Macromolecules* **2003**, *36*, 3635−3645.
(9) Mijovic, J.; Shen, M.; Sy, J. W.; Mondragon, I. *Macromolecules* **2000**, *33*, 5235−4244.
(10) Dean, J. M.; Lipic, P. M.; Grubbs, R. B.; Cook, R. F.; Bates, F. S. *J. Polym. Sci., Part B: Polym. Phys.* **2001**, *39*, 2996−3010.
(11) Ritzenthaler, S.; Court, F.; David, L.; Girard-Reydet, E.; Leibler, L.; Pascault, J. P. *Macromolecules* **2002**, *35*, 6245−6254.
(12) Ritzenthaler, S.; Court, F.; David, L.; Girard-Reydet, E.; Leibler, L.; Pascault, J. P. *Macromolecules* **2003**, *36*, 118−126.
(13) Dean, J. M.; Verghese, N. E.; Pham, H. Q.; Bates, F. S. *Macromolecules* **2003**, *36*, 9267−9270.

(14) Kinloch, A. J.; Shaw, S. J.; Tod, D. A.; Hunston, D. L. *Polymer* **1983**, *24*, 1341−1354.
(15) Cardwell, B. J.; Yee, A. F. *J. Mater. Sci.* **1998**, *33*, 5473−5484.
(16) Xu, Z.; Hameed, N.; Guo, Q.; Mai, Y.-W. *J. Appl. Polym. Sci.* **2010**, *115*, 2110−2118.
(17) Larrañaga, M.; Gabilondo, N.; Kortaberria, G.; Serrano, E.; Remiro, P.; Riccardi, C. C.; Mondragon, I. *Polymer* **2005**, *46*, 7082−7093.
(18) Larrañaga, M.; Arruti, P.; Serrano, E.; de la Caba, K.; Remiro, P.; Riccardi, C. C.; Mondragon, I. *Colloid Polym. Sci.* **2006**, *284*, 1419−1430.
(19) Meng, F.; Zheng, S.; Zhang, W.; Li, H.; Liang, Q. *Macromolecules* **2006**, *39*, 711−719.
(20) Ocando, C.; Serrano, E.; Tercjak, A.; Peña, C.; Kortaberria, G.; Calberg, C.; Grignard, B.; Jerome, R.; Carrasco, P. M.; Mecerreyes, D.; Mondragon, I. *Macromolecules* **2007**, *40*, 4068−4074.
(21) Meng, F.; Xu, Z.; Zheng, S. *Macromolecules* **2008**, *41*, 1411−1420.
(22) Hillmyer, M. A.; Lipic, P. M.; Hadjuk, D. A.; Almdal, K.; Bates, F. S. *J. Am. Chem. Soc.* **1997**, *119*, 2749−2750.
(23) Cicala, G.; Mamo, A.; Recca, G.; Restuccia, C. L. *Polym. Eng. Sci.* **2007**, *47*, 2027−2033.
(24) Ritzenthaler, S.; Court, F.; David, L.; Girard-Reydet, E.; Leibler, L.; Pascault, J. P. *Macromolecules* **2002**, *35*, 6245−6254.
(25) Rebizant, V.; Abetz, V.; Tournilhac, F.; Court, F.; Leibler, L. *Macromolecules* **2003**, *36*, 9889−9896 (2003).
(26) Hermel-Davidock, T. J.; Tang, H. S.; Murray, D. J.; Hahn, S. F. *J. Polym. Sci., Part B: Polym. Phys.* **2007**, *45*, 3338−3348.
(27) Dean, J. M.; Grubbs, R. B.; Saad, W.; Cook, R. F.; Bates, F. S. *J. Polym. Sci., Part B: Polym. Phys.* **2003**, *41*, 2444−2456.
(28) Rebizant, V.; Venet, A. S.; Tournilhac, F.; Girard-Reydet, E.; Navarro, C.; Pascault, J. P.; Leibler, L. *Macromolecules* **2004**, *37*, 8017−8027.
(29) Wu, J.; Thio, Y. S.; Bates, F. S. *J. Polym. Sci., Part B: Polym. Phys.* **2005**, *43*, 1950−1965.
(30) Thio, Y. S.; Wu, J.; Bates, F. S. *Macromolecules* **2006**, *39*, 7187−7189.
(31) Larrañaga, M.; Serrano, E.; Martin, M. D.; Tercjak, A.; Kortaberria, G.; de la Caba, K.; Riccardi, C. C.; Mondragon, I. *Polym. Int.* **2007**, *56*, 1392−1403.
(32) Grubbs, R. B.; Dean, J. M.; Broz, M. E.; Bates, F. S. *Macromolecules* **2000**, *33*, 9522−9534.
(33) Fan, W.; Wang, L.; Zheng, S. *Macromolecules* **2009**, *42*, 327−336.
(34) Hameed, N.; Guo, Q.; Xu, Z.; Hanley, T. L.; Mai, Y.-W. *Soft Matter* **2010**, *6*, 6119−6129.
(35) Fan, W.; Wang, L.; Zheng, S. *Macromolecules* **2010**, *43*, 10600−10611.
(36) Jian, X.; Hay, A. S. *J. Polym. Sci., Part A: Polym. Chem.* **1991**, *29*, 1183−1189.
(37) Ocando, C.; Tercjak, A.; Serrano, E.; Ramos, J. A.; Corona-Galván, S.; Parellada, M. D.; Fernández-Berridi, M. J.; Mondragon, I. *Polym. Int.* **2008**, *57*, 1333−1342.
(38) Serrano, E.; Tercjak, A.; Ocando, C.; Larrañaga, M.; Parellada, M. D.; Corona-Galván, S.; Mecerreyes, D.; Zafeiropoulos, N. E.; Stamm, M.; Mondragon, I. *Macromol. Chem. Phys.* **2007**, *208*, 2281−2292.
(39) Serrano, E.; Tercjak, A.; Kortaberria, G.; Pomposo, J. A.; Mecerreyes, D.; Zafeiropoulos, N. E.; Stamm, M.; Mondragon, I. *Macromolecules* **2006**, *39*, 2254−2261.
(40) Gutierrez, J.; Tercjak, A.; Mondragon, I. *J. Phys. Chem. C* **2010**, *114*, 22424−22430.
(41) Lazzari, M.; Scalarone, D.; Vazquez-Vazquez, C.; López-Quintela, M. A. *Macromol. Rapid Commun.* **2008**, *29*, 352−357.
(42) Choucair, A.; Eisenberg, A. *Eur. Phys. J. E* **2003**, *10*, 37−44.
(43) Bhargava, P.; Zheng, J. X.; Li, P.; Quirk, R. P.; Harris, F. W.; Cheng, S. Z. D. *Macromolecules* **2006**, *39*, 4880−4888.
(44) Cho, H.; Park, H.; Park, S.; Choi, H.; Huang, H.; Chang, T. *J. Colloid Interface Sci.* **2011**, *356*, 1−7.
(45) Ocando, C.; Tercjak, A.; Martín, M. D.; Ramos, J. A.; Campo, M.; Mondragon, I. *Macromolecules* **2009**, *42*, 6215−6224.
(46) Hameed, N.; Guo, Q.; Hanley, T.; May, Y.-W. *J. Polym. Sci., Part B: Polym. Phys.* **2010**, *48*, 790−800.